Decoupling single nanowire mobilities limited by surface scattering and bulk impurity scattering

D. R. Khanal,[1,2] A. X. Levander,[1,2] K. M. Yu,[2] Z. Liliental-Weber,[2] W. Walukiewicz,[2] J. Grandal,[3] M. A. Sánchez-García,[3] E. Calleja,[3] and J. Wu[1,2,a)]
[1]*Department of Materials Science and Engineering, University of California, Berkeley, California 94720, USA*
[2]*Materials Science Division, Lawrence Berkeley National Laboratory, Berkeley, California 94720, USA*
[3]*Department of Ingeniería Electrónica-ISOM, Universidad Politécnica, Ciudad Universitaria, 28040 Madrid, Spain*

(Received 15 February 2011; accepted 7 June 2011; published online 2 August 2011)

We demonstrate the isolation of two free carrier scattering mechanisms as a function of radial band bending in InN nanowires via universal mobility analysis, where effective carrier mobility is measured as a function of effective electric field in a nanowire field-effect transistor. Our results show that Coulomb scattering limits effective mobility at most effective fields, while surface roughness scattering only limits mobility under very high internal electric fields. High-energy α particle irradiation is used to vary the ionized donor concentration, and the observed decrease in mobility and increase in donor concentration are compared to Hall effect results of high-quality InN thin films. Our results show that for nanowires with relatively high doping and large diameters, controlling Coulomb scattering from ionized dopants should be given precedence over surface engineering when seeking to maximize nanowire mobility. © *2011 American Institute of Physics*. [doi:10.1063/1.3611032]

I. INTRODUCTION

Successful realization of useful device applications from nanoscale semiconductors necessitates a comprehensive understanding of their electronic properties, in particular, carrier mobility, which is more difficult to directly engineer than carrier concentration, yet is equally critical to controlling dc and high-frequency conductivity. Specifically, the large surface-to-volume ratio of many nanoscale semiconductors has led to increased interest on the impact of surface roughness scattering on the overall carrier mobility. This is especially true for semiconductor nanowires, which, as a result of intense research over the past two decades, have shown promise in a variety of topical applications, including photovoltaics,[1] energy storage,[2] and sensing,[3] to name a few. Nevertheless, detailed experimental results distinguishing between different scattering mechanisms that limit nanowire carrier mobility have been rarely reported. Moreover, a correlation between free carrier scattering mechanism and free carrier distribution within nanowires was most often discussed only qualitatively, despite the fact that applied gate fields can significantly affect both carrier distribution throughout the cross-section of a nanowire and the relative importance of different scattering mechanisms. In this work, we demonstrate a way to quantify different electron scattering mechanisms in single nanowires.

For temperature ranges where shallow dopants are fully ionized, the dominant free carrier scattering mechanisms are Coulomb scattering from ionized impurities, phonon scattering, and surface roughness scattering. The mobility (μ) limited by these different scattering mechanisms is described by

$$\frac{1}{\mu} = \frac{1}{\mu_C} + \frac{1}{\mu_{ph}} + \frac{1}{\mu_{sr}}, \tag{1}$$

where μ_C is the Coulomb scattering limited mobility, μ_{ph} is the phonon scattering limited mobility, and μ_{sr} is the surface roughness scattering limited mobility.

In contrast to bulk semiconductors where mobility can be measured via the Hall effect, the mobility of single nanowires is most often deduced from field-effect transistor (FET) measurements. Mobility can be defined in two ways from FET measurements:[4] field-effect mobility (μ_{FE}) and effective mobility (μ_{eff}). The field-effect mobility is proportional to the slope of the current (I_{sd}) versus gate voltage (V_g) curve, i.e., transconductance ($g_m = \partial I_{sd}/\partial V_g$). For a nanowire,

$$\mu_{FE} = \frac{g_m L^2}{C V_{sd}}, \tag{2}$$

where C is the gate-nanowire capacitance, L is the channel length, and V_{sd} is the source-drain voltage. In contrast, the effective mobility is given by

$$\mu_{eff} = \frac{I_{sd} L^2}{V_{sd} C (V_g - V_{th})}, \tag{3}$$

where V_{th} is the threshold gate voltage, which often has a range of uncertainty and qualitatively corresponds to the gate voltage required to induce strong inversion (inversion-mode FETs) or accumulation (accumulation-mode FETs).

a)Author to whom correspondence should be addressed. Electronic mail: wuj@berkeley.edu.

 © 2011 American Institute of Physics

Downloaded 02 Aug 2011 to 128.32.121.22. Redistribution subject to AIP license or copyright; see http://jap.aip.org/about/rights_and_permissions

Notably, although μ_{eff} is the more accurate predictor of device characteristics such as source-drain current, μ_{FE} has been most often used for nanowire characterization, presumably due to uncertainty in defining V_{th}. However, at gate voltages greater (e.g., more positive when accumulating electrons) than where the transconductance peaks, μ_{FE} is always lower than μ_{eff} and is not as physically meaningful.[4]

Nonetheless, μ_{FE} has been used to probe the impact of surface roughness scattering in semiconductor nanowires by several groups,[5–7] who have observed a decrease in peak μ_{FE} with decreasing nanowire diameter, attributed to an increase in surface roughness scattering with decreasing nanowire diameter. However, this technique of measuring peak μ_{FE} as a function of nanowire diameter does not allow one to quantify the magnitudes of different scattering mechanism at the single nanowire level, nor does it address the effects of radial carrier distribution and band-bending on dictating which scattering mechanisms dominate. Moreover, these studies implicitly assume that nanowires with different diameters have equal dopant concentrations and uniform dopant distributions, which requires independent testing given the complications of dopant distribution[8,9] and incorporation[10] in nanowires.

The issue of radial carrier distribution is especially significant in nanowires due to their small size. For example, significant effects on the electronic and optical properties of nanowires have been attributed to the intrinsic surface band bending of different semiconductors.[11–13] Band bending and radial carrier distributions in nanowires can be affected by a variety of growth and post-processing parameters, including doping conditions, surface treatments, and alloying. Most importantly, the carrier profile can be significantly modified *during* device operation in various applications, for example, by the adsorption of chemical species in nanowire sensors,[3] or most dramatically, by an applied electric field in an FET.[14] In all of these situations, a slight change in band bending can dictate whether the majority of free carriers are located within a few nanometers of the surface or shielded from the surface by a depletion region. A difference in surface versus core mobilities can thus appreciably affect device current. This is in contrast with bulk and thin-film semiconductors where current often flows many microns from the surface, and as a result, differences in surface and core mobilities often have little effect on the overall measured current. Therefore, the common practice of assigning *one* peak μ_{FE} to a single nanowire, irrespective of internal electric fields, is an incomplete description of nanowire conduction; an experimental method to quantitatively distinguish between different scattering mechanisms as a function of band bending at the single nanowire level is desirable for both a better fundamental understanding of nanowire conduction as well as for improved nanowire device engineering.

Fortunately, the issue of mobility dependence on band bending and carrier distribution has been studied in detail for Si-based metal oxide FETs (MOSFETs). In particular, Sabnis and Clemens[15] observed that when the channel effective mobility is plotted versus the average (or "effective") electric field (E_{eff}) in the inversion layer, the mobilities of samples with different background dopant concentrations merge onto a single curve, referred to as the universal mobility curve. Further studies by multiple groups found that three distinct regimes were present in the universal mobility curve of inversion-mode MOSFETs: an upward slope at low effective fields ascribed to mobility limited by Coulomb scattering, a shallow downward slope at slightly higher effective fields ascribed to phonon scattering, and a steeper downward slope at the highest effective fields ascribed to surface roughness scattering,[16] as shown schematically in Fig. 1. The universal mobility curves for accumulation-mode MOSFETs with different channel doping are identical except for the low-field Coulomb scattering regime, where μ_{eff} is constant with respect to electric field due to the screening of ionized impurities by majority carriers even at near-zero electric fields.[17] Since phonon and surface roughness scattering are independent of dopant concentration, the mobilities of MOSFETs with different dopant concentrations merge toward the same values at high E_{eff}, giving the mobility curves their "universal" behavior. This behavior was subsequently used by multiple groups to extract detailed information regarding carrier scattering as a function of electric field in MOSFETs, including distinguishing between different scattering mechanisms.[16] Despite the abundance of FET experiments performed on nanowires, to our knowledge, an analysis of nanowire effective mobility as a function of internal electric field aimed at distinguishing between different scattering mechanisms has yet to be reported. In this paper, using InN nanowires as an example material in careful comparison to InN thin films, we separate the effects of surface roughness scattering from other scattering mechanisms in individual semiconductor nanowires following universal mobility analysis.

InN was chosen due to its naturally strong surface electron accumulation, which makes it sensitive to surface electrostatics without the need for extreme gate voltages.[18] In addition, surround-gating of InN nanowires, as used here, avoids the complication inherent to InN thin film experiments of having to decouple front surface conduction from

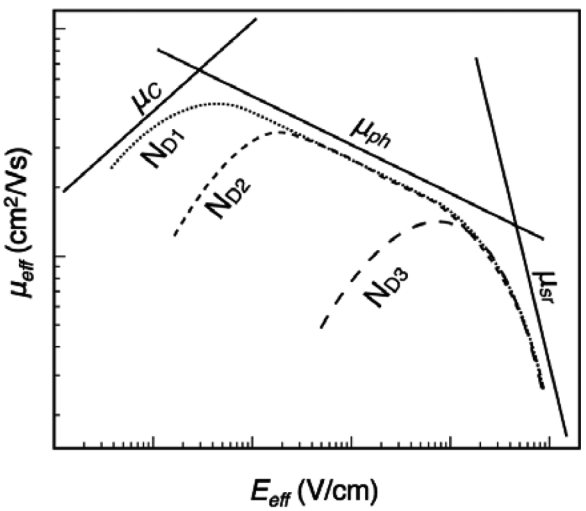

FIG. 1. Schematic of typical Si MOSFET universal mobility curves where μ_{eff} is plotted as a function of E_{eff} on a log-log scale for three background dopant concentrations ($N_{D1} < N_{D2} < N_{D3}$). Solid lines show mobilities limited by Coulomb, phonon, and surface roughness scattering.

Downloaded 02 Aug 2011 to 128.32.121.22. Redistribution subject to AIP license or copyright; see http://jap.aip.org/about/rights_and_permissions

back-interface (film to substrate) conduction, the electronics of which are poorly understood.[19] The InN nanowires were grown by molecular-beam epitaxy (MBE), as described in Ref. 39. Nanowire FETs were fabricated by detaching them from their growth substrate by ultrasonication in 2-propanol, followed by dropcasting onto a 200 nm SiN-on-Si chip for device fabrication by electron-beam lithography. The contact metals (20 nm Ti/120 nm Au) were deposited by electron-beam evaporation.

For the nanowires studied (diameters 30–50 nm), our results indicate that carrier scattering is dependent on band bending in the wire but that surface roughness scattering limits free carrier mobility only at high surface fields, consistent with Si MOSFET behavior. The results suggest that for most semiconductor nanowires with diameters equal or larger than these, surface roughness scattering will not limit mobility except for at large applied fields. This implies that controlling Coulomb scattering from ionized dopants should be given precedence over surface treatments when optimizing nanowire mobility. The results also emphasize the importance of considering band bending and Fermi-level pinning when quantifying the electrical properties of semiconductor nanowires, which are particularly sensitive to surface effects.

II. EXPERIMENTAL DETAILS

Both InN nanowires[20] and InN thin films[21] consistently display heavily doped n-type behavior, due to an intrinsically high donor-like point-defect density ($\sim 10^{17} - 10^{20}$ cm^{-3}). In addition, it has been recently confirmed by several groups[13,20,22] that InN nanowires with non-polar sidewalls display strong surface Fermi-level (E_F) pinning at $\sim$0.9 eV above the conduction band minimum (E_{CB}), which results in a heavy electron accumulation layer, similar to InN thin films. This is convenient for universal mobility analysis because large internal electric fields are experimentally accessible with only moderate applied gate voltages. Electrolyte gating, where the gate voltage is applied to an electrolyte in $\sim 360^{o}$ contact with the semiconductor was used, due to its higher gate-nanowire capacitances compared to solid gating.[23] When a gate voltage is applied, ions in the electrolyte ($KClO_4^-$ in 1000 MW polyethylene oxide with a [K]:[O] ratio of 100:1) are driven toward or away from the semiconductor surface depending on V_g polarity, modulating current in the semiconductor. By holding the gate voltage to within a certain range (+/−2 V in our case), this charge modulation can be achieved without appreciable leakage current between the electrolyte and the semiconductor. Electrical measurements were performed at 50 °C, which is above the melting point of the polyethylene oxide (PEO) electrolyte, to minimize hysteresis in the current versus gate voltage curves. The dopant concentration of individual nanowires was varied by irradiation with 2 MeV α particles at fluences between 2×10^{14} cm^{-2} to 2×10^{15} cm^{-2}, which has been shown to increase the donor-like point defect concentration in InN thin films.[21,24,25] Multiple irradiation steps were done on a single device chip allowing us to measure the same nanowires with a range of controlled donor concentrations.

III. RESULTS AND DISCUSSION

Figure 2 shows $I_{sd}(V_g)$ curves of a typical InN nanowire as a function of irradiation dose (Data from 5 nanowires were recorded for every irradiation fluence). A droplet of the PEO electrolyte was placed on the device chip for a short time after each irradiation to measure the $I_{sd}(V_g)$ behavior and then immediately dissolved and rinsed in de-ionized water, so each irradiation step was performed with no PEO droplet covering the wires. To ensure that the changes in $I_{sd}(V_g)$ were due to irradiation and not consecutive rinsing and reapplication of PEO droplets, $I_{sd}(V_g)$ curves of multiple devices were measured using consecutive PEO droplets without an irradiation step in between. This is shown, for example, at the fluence of 2.1×10^{14} cm^{-2} for the device in Fig. 2; the difference in these two curves is negligible compared to the effect of irradiation.

The fact that the nanowires are systematically harder to deplete with increased irradiation dose is consistent with the expectation of a larger donor concentration with increasing irradiation fluence. In order to quantify this effect, we fit computed $I_{sd}(V_g)$ curves to the experimental $I_{sd}(V_g)$ data via finite element simulations of the electrostatics of a given nanowire. This method for quantifying the extent of surface Fermi-level pinning in nanowires is described in detail in Ref. 20. Briefly, the theoretical $I_{sd}(V_g)$ curves are computed using a Drude model of conductivity, allowing the electron concentration to be a function of radial position across the nanowire. This radial electron distribution, $n(r)$, is computed by solving Poisson's equation in three-dimensions via finite element analysis using a classical 3D density of states. Since $n(r)$ is a function of the donor concentration (N_D) and Fermi-level pinning energy ($E_{pin} = E_F - E_{CB}$), $I_{sd}(V_g)$ curves for a range of E_{pin} and N_D can be computed and fit to the

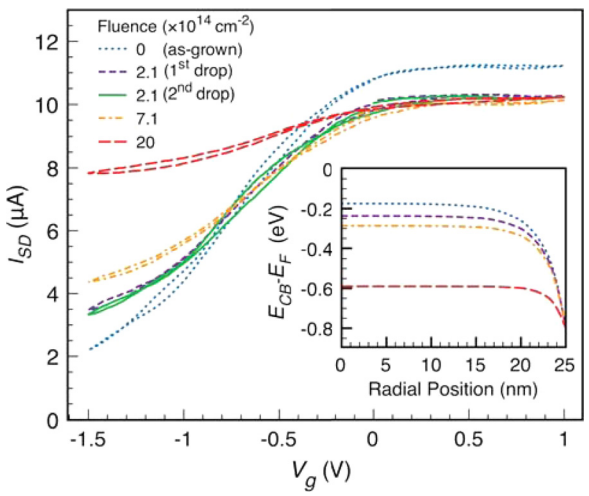

FIG. 2. (Color online) Experimental electrolyte-gated $I_{sd}(V_g)$ curves as a function of α particle irradiation fluence from a typical InN nanowire device. For all curves, V_g was swept from 0 to −1.5 to 1 V and back to 0 V at a rate of 20 mV/sec. Inset: Conduction band energy profiles relative to the Fermi-level (E_F) as a function of radial position (r) in the nanowire at $V_g = 0$ from fits to the as-grown and irradiated curves (same legend as main). Nanowire core is at 0 nm and surface is at 25 nm. The N_D values corresponding to the as-grown, 2.1×10^{14} cm^{-2}, 7.1×10^{14} cm^{-2}, 2.0×10^{15} cm^{-2} fluences are 7×10^{18} cm^{-3}, 1.2×10^{19} cm^{-3}, 1.7×10^{19} cm^{-3}, and 7×10^{19} cm^{-3}, respectively.

Downloaded 02 Aug 2011 to 128.32.121.22. Redistribution subject to AIP license or copyright; see http://jap.aip.org/about/rights_and_permissions

experimental $I_{sd}(V_g)$ curves to find the E_{pin} and N_D that best fit the data. Such fitting was performed on three nanowires in this study. Radial conduction band profiles corresponding to increases in N_D by irradiation are shown in the inset of Fig. 2.

The change in N_D with fluence for all three nanowires is plotted in Fig. 3 along with the behavior of irradiated InN thin films.[25,26] We see that although the as-grown nanowires start with a slightly higher N_D than the InN films, upon irradiation, N_D is dictated by irradiation fluence, evidenced by the agreement between our nanowire data and the InN thin films from Refs. 25 and 26 which were measured by Hall effect. This agreement confirms that high-energy particle irradiation increases the donor-like native defect concentration in InN nanowires in the same fashion as in thin films. The Fermi level pinning position that best fit the experimental data for all wires and doses was 0.8 +/− 0.1 eV (Fig. 2 inset), in agreement with previous results in Ref. 20.

Previous reports[27,28] on the effects of 10 MeV proton irradiation on back-gated ZnO nanowire and carbon nanotube FETs attributed changes in $I_{sd}(V_g)$ behavior to irradiation-induced trapped charges in their gate dielectric (SiO_2) and nanowire-dielectric interface. In this work, the excellent agreement of our N_D versus fluence data with InN thin films, combined with a consistent E_{pin} extracted from all wires at all doses, confirms that the changes in our $I_{sd}(V_g)$ data are due to native defect generation and not trapped charges in the nitride or nanowire-nitride interface. If trapped charges in the silicon nitride substrate were responsible, we would have observed a change in E_{pin}, not N_D, as a function of irradiation fluence. The discrepancy between our results and that of Refs. 27 and 28 could be due to several factors, but primarily, silicon nitride is known to be resistant to radiation-induced changes in electrical behavior, unlike silicon oxide.[29,30] In addition, differences in gate geometry (surround versus back) and ion energy (10 MeV versus 2 MeV) may have also contributed to this discrepancy.

After quantifying the various electrostatic variables in the nanowire [N_D, E_{pin}, electric potential φ, $n(r)$], the effective mobility and effective field were calculated as follows. The effective field is defined as the weighted average electric field experienced by accumulated electrons.[4] For a surround-gated cylindrical nanowire,

$$E_{eff}(V_G) = \frac{\int_0^R n(r, V_G)E(r)rdr}{\int_0^R n(r, V_G)rdr}, \quad (4)$$

where $E(r)$ is the radial component of the electric field in the nanowire, and R is the nanowire radius. Since, by definition, the electric field is non-zero only in the accumulation region, μ_{eff} is defined as the effective mobility for only the accumulated electrons, that is, the average electron concentration (n_{ave}) in excess of the background dopants, yielding the following equation for current:

$$I_{SD}(V_G) - I_0 = \left[n_{ave}(V_G) - n_{ave}^0\right]\frac{\pi R^2}{L} q\mu_{eff} V_{SD}\,, \quad (5)$$

where $n_{ave}^0 = N_D$ is the electron concentration from dopants, which explicitly excludes electrons induced by band bending (i.e., "flatband" electron concentration). Likewise, I_0 is the flatband current [$I_0 = I_{sd}(V_g = V_{FB})$]. In all cases, V_{sd} was modified to account for contact resistance (R_c) via $V_{tot} = V_{sd} + IR_c$, where V_{tot} is the total voltage drop applied between the source and drain electrodes.[31]

Figure 4 shows μ_{eff} as a function of E_{eff} for a range of irradiation fluences. Similar to the universal mobility curves of accumulation-mode MOSFETs, we see a clear distinction between a flat μ_{eff} regime at low E_{eff}, generally ascribed to the Coulomb scattering limited regime, and a sharp drop in μ_{eff} at high E_{eff}, ascribed to surface roughness scattering. Calculations of InN mobilities near room temperature have shown that for N_D above mid-10^{18} cm^{-3}, phonon scattering

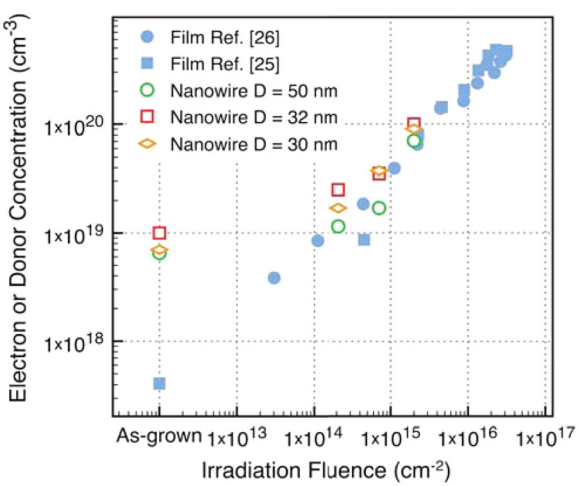

FIG. 3. (Color online) Extracted N_D vs irradiation fluence of three InN nanowires of various diameters (D) from this study, plotted with electron concentration vs fluence of InN thin films from Refs. 25 and 26.

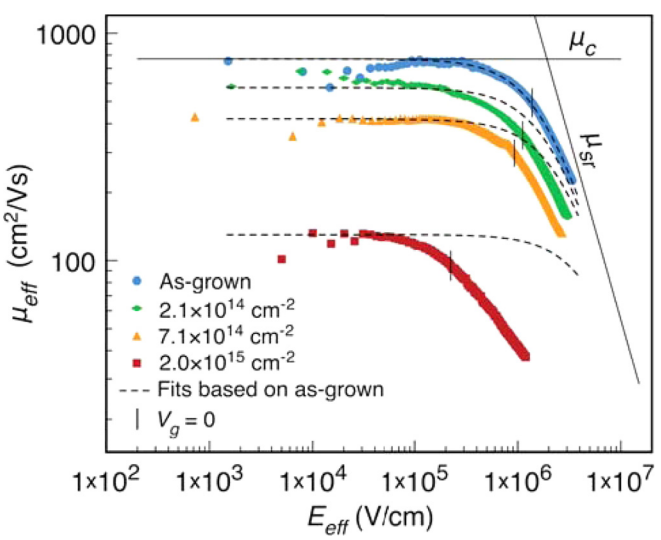

FIG. 4. (Color online) Effective electron mobility as a function of effective electric field for a series of irradiation fluences of the InN nanowire device from Fig. 2. Dashed lines show fits using Eq. 1 where μ_c is adjusted to fit the low-field mobility from each irradiation fluence while μ_{sr} (Eq. 6) is held fixed for all fluences and $\beta = 8.6 \times 10^{12}$ ($cm^{2-\gamma}$ $V^{\gamma-1}$ s^{-1}) and $\gamma = 1.6$ are chosen to only fit the as-grown mobility data. Solid lines show the μ_c and μ_{sr} functions used for the fit to the as-grown mobility data. Short vertical lines indicate the E_{eff} values that correspond to $V_g = 0$.

Downloaded 02 Aug 2011 to 128.32.121.22. Redistribution subject to AIP license or copyright; see http://jap.aip.org/about/rights_and_permissions

is not a limiting factor[32] and was thus not included in fits to the mobility curves as discussed below. To gauge what scattering processes limit nanowire mobility under no applied field, the electric fields corresponding to zero gate voltage ($V_g = 0$ V) are marked for each mobility curve in Fig. 4. For our nanowires, μ_{eff} at $V_g = 0$ V is in a transition regime where both surface roughness and Coulomb scattering contribute to limiting electron mobility. As discussed earlier, however, InN has unique surface Fermi-level pinning that gives it an unusually high internal electric field even at $V_g = 0$ V. In most semiconductors such as Si and GaAs, the surface Fermi level is pinned near the middle of the bandgap,[33] which results in much smaller surface band bending or even a slight surface depletion. In these low-field conditions, Fig. 4 predicts that μ_c will dominate over μ_{sr} for nanowires with dopant concentrations ($> 10^{18}$ cm^{-3}) and diameters (> 30–50 nm) comparable to those in our work. For more lightly doped semiconductors, μ_{eff} at low E_{eff} may be limited by μ_{ph} rather than μ_c. Thus, *a priori* assumptions about conduction in semiconductor nanowires being limited by surface roughness should be questioned. For smaller diameter nanowires, where quantum confinement begins to significantly affect both the density of states and the wavefunctions of the electrons, the strictly classical approach as presented here does not apply and quantum mechanical considerations are necessary. Our calculations indicate that confinement-induced singularities in the InN density of states for nanowires of 30–50 nm will have energy spacings between 4 and 11 meV, well below k_BT in our experimental condition (30 meV), and can therefore be approximated by a classical density of states.

To further confirm that Coulomb and surface roughness scattering are the limiting factors of mobility at low and high fields, respectively, we fit the $\mu_{eff}(E_{eff})$ data with Eq. 1 (Fig. 4). As explained earlier, μ_c is a constant with respect to E_{eff} for accumulation-mode FETs, while the surface roughness scattering limited mobility is empirically known to depend on E_{eff} as[16]

$$\mu_{sr} = \beta E_{eff}^{-\gamma}, \tag{6}$$

where γ is generally 2 (at low temperatures) and the coefficient β is inversely dependent on material parameters such as effective mass and surface roughness. Looking first at the as-grown mobility curve in Fig. 4, we see that an excellent fit can be obtained with just μ_c and μ_{sr}, without including μ_{ph}, consistent with the expectation of a minimal influence from phonon scattering at these donor concentrations. Also shown in Fig. 4 are fits to the mobility data recorded after the three irradiation fluences. In these fits, μ_c is adjusted to best fit the flat low-field regime for each fluence (to account for the increase in N_D with increasing irradiation fluence) but $\mu_{sr}(E_{eff})$ is kept fixed using the β and γ values that best fit the as-grown mobility curve. Clearly, a single $\mu_{sr}(E_{eff})$ function cannot describe the high-field mobility behavior from all irradiation fluences, suggesting that in addition to increasing the ionized donor concentration, high-energy ion irradiation may also effect the surface roughness of these nanowires, as discussed below. In order to confirm that the reduction in μ_c with fluence is due to an increase in N_D, we compare our results with Hall mobility measurements of as-grown, α particle irradiated, and electrolyte-gated InN thin films.

A decrease in Hall mobility with increasing donor concentration (N_D) from high-energy α particle irradiation has been well documented for InN thin films.[24–26] Specifically, Hall mobilities of irradiated InN films as a function of electron concentration have been shown to agree very well with theoretical calculations of mobility limited by triply charged donors. In Fig. 5 we plot our μ_c versus N_D for three nanowires along with the InN thin-film Hall mobility data from Ref. 25. Because the Hall effect technique samples a large portion of the interior of a film, the Hall mobility of InN thin films is limited by Coulomb scattering (at these high dopant concentrations), not surface roughness scattering, and is therefore comparable to the μ_c values of our nanowires. We see that our μ_c versus N_D data agree with the thin film data, confirming that the native defects created by irradiation in our nanowires are largely the same as those in InN thin films.

Next, we turn to surface roughness limited mobility. By comparing Figs. 2 and 4, we see that the decrease in μ_{eff} at high fields corresponds to a decrease in transconductance at more positive V_g. Although a decrease in the transconductance of an FET at accumulation voltages can be caused by FET-specific factors,[34] it is worthwhile to note that a similar decrease in mobility at accumulation voltages has been observed in InN thin films in electrolyte-gated Hall effect measurements, where an increase in surface scattering was qualitatively cited as the likely cause of the decrease.[19] The agreement of those Hall mobility results with the high-field μ_{eff} decrease in this work strongly suggests that surface scattering, not FET device artifacts, are responsible for the decrease in transconductance observed at high E_{eff} in our nanowires.

Upon α particle irradiation, we expect that while μ_c reduces as a result of the increase in N_D, μ_{sr} will remain

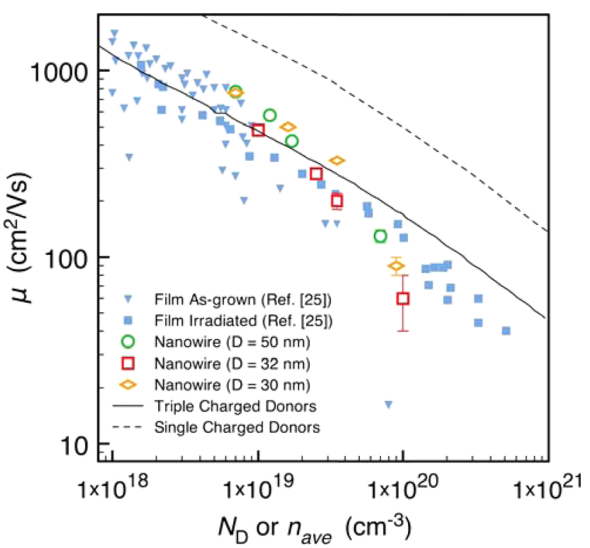

FIG. 5. (Color online) Hall mobility vs electron concentration (n_{ave}) of InN thin films from Ref. 25 plotted with μ_c vs N_D of three nanowires from this work. Also shown are theoretically calculated mobilities limited by triple and single charged defects in InN from Ref. 26.

Downloaded 02 Aug 2011 to 128.32.121.22. Redistribution subject to AIP license or copyright; see http://jap.aip.org/about/rights_and_permissions

unchanged, resulting in the universal mobility behavior similar to Si MOSFETs at high effective fields. However, Fig. 4 shows that a single μ_{sr} cannot describe the high-field behavior of all of the curves; each of the first three mobility curves (as-grown, 2.1×10^{14} cm^{-2} and 7.1×10^{14} cm^{-2}) can be fit independently by reducing β while keeping γ constant.[35] To elucidate this lack of mobility universality at high fields, an understanding of the dependence of β on material parameters is necessary. Lee *et al.*[36] state that β is inversely proportional to the effective mass (m_{eff}) and surface roughness as per

$$\beta \propto \frac{1}{m_{eff}(L\Delta)^2}, \tag{7}$$

where L and Δ are the correlation length and mean asperity height of the semiconductor surface, respectively, which are two parameters used to characterize surface roughness. The β values that fit the mobility curves for the first two irradiation fluences, 2.1×10^{14} cm^{-2} and 7.1×10^{14} cm^{-2}, differ from the β value of the as-grown curve by 44% and 60%, respectively.

The effective mass of electrons is indeed expected to increase with increasing irradiation fluence as a result of the non-parabolicity of the conduction band minimum of InN. However, from the known dependence of m_{eff} on conduction band population in InN thin films,[18] the maximum expected change in m_{eff} in our nanowires resulting from irradiation is 8%. Thus, effective mass changes alone cannot explain the lack of universal mobility behavior at high fields.

A possible explanation for the decrease in β is that the 2 MeV α particle irradiation, besides increasing the native defect concentration in InN, also increases its surface roughness. Although sputtering or etching of semiconductors and metals by high energy ions is generally considered to be weak at MeV energies, Eq. 7 suggests that only a slight increase in surface roughness is sufficient to account for our observed changes in β. For example, if Δ in an as-grown nanowire is $\approx$1 nm, an increase in Δ of only 6 Å to 1.6 nm upon irradiation would fully account for the observed 60% change in β. Changes in surface morphology after irradiation with ions of MeV energies have, in fact, been reported in the literature. Maaza *et al.*[37] reported changes in indium tin oxide surface morphology after irradiation with 2 MeV He^+ ions with fluences comparable to this work (2×10^{15}–6×10^{15} cm^{-2}). In addition, a monotonic increase in surface roughness of zirconia films irradiated with 250–450 keV He^+ ions was found with atomic force microscopy (AFM) by Kuri *et al.*[38] The rms roughness of these samples increased from 0.17 to 0.4 nm.

As AFM measurements of single nanowire surface roughness are difficult, to investigate the change in surface morphology with irradiation, we performed high-resolution transmission electron microscopy (TEM) on as-grown and irradiated (2×10^{15} cm^{-2}) nanowires. Bright-field images of a large number of nanowires indicated that the vast majority of wires were largely free of extended defects (e.g., dislocations, stacking faults), consistent with previous reports.[22] High-resolution phase contrast images were obtained from many regions along the length of nanowires from both the as-grown and irradiated samples (Fig. 6). We observed a systematic difference in amorphous layer thickness as well as InN surface roughness between the two samples. Amorphous oxide layers in the as-grown nanowires were limited in thickness to less than 1–2 nm and appeared sporadically throughout the length of any given wire. The interface between the amorphous layer (if any) and the crystalline InN is extremely smooth [Fig. 6(a)]. In contrast, amorphous oxide layers were observed to be thicker and more frequent along the length of irradiated wires [Fig. 6(b)]. Though the irradiation was performed under vacuum (5×10^{-6} Torr), it is possible that lattice damage at the surface due to irradiation leads to oxidation immediately upon exposure to ambient. A comparison between Figs. 6(a) and 6(b) suggests the interface roughness may be enhanced after irradiation, although a quantitative correlation of the surface or interface roughness to irradiation requires systematic investigations under better controlled conditions. Lastly, it is possible that an increased oxide thickness decreases the efficiency of gating by effectively increasing the Helmholtz layer (i.e., "gate dielectric") thickness during electrolyte-gating. However, such an effect would reduce gating efficiency at all gate voltages, not simply at large positive gate voltages that correspond to the high-E_{eff} regime in discussion.

IV. SUMMARY

We have presented a technique for quantifying the magnitude of individual scattering mechanisms that limit carrier mobility in semiconductor nanowires. Using well-established universal mobility analysis, which involves examining the dependence of effective mobility on effective electric field in a gated semiconductor, we were able to distinguish between Coulomb scattering limited mobility at low-fields and surface roughness limited mobility at high fields using MBE-grown crystalline InN nanowires as an example material. Our results show that for InN nanowires with diameters between 30–50 nm, surface roughness scattering only limits carrier mobility when there is heavy band bending near the

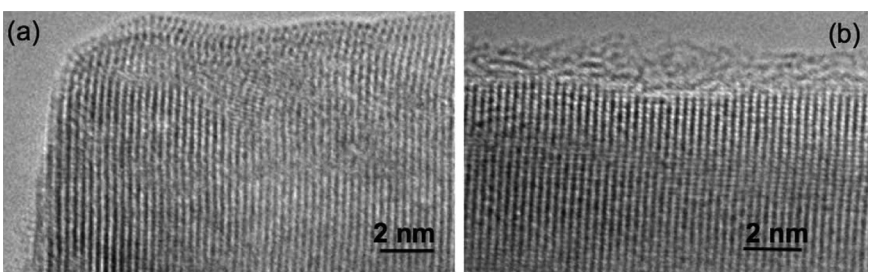

FIG. 6. High-resolution TEM micrographs of as-grown (a) and irradiated (b) InN nanowires. The edges on all images are the sidewalls of the nanowires. Scale bars are 2 nm.

Downloaded 02 Aug 2011 to 128.32.121.22. Redistribution subject to AIP license or copyright; see http://jap.aip.org/about/rights_and_permissions

surface of the wire ($\approx 10^6$ V/cm), which occurs naturally in InN, but not in most other semiconductors. This implies that for semiconductor nanowires where quantum confinement is not significant, scattering from ionized dopants or phonons rather than from surface roughness will limit the mobility except at large internal electric fields.

These results have important device implications. Namely, for high-mobility applications, optimizing dopant and defect concentrations should be given priority over surface engineering. We note that it is not possible to separate different scattering mechanisms as a function of band bending in individual nanowires using the common technique of comparing peak field-effect mobilities between different nanowires. This μ_{eff} versus E_{eff} analysis should thus be exploited for future studies of, for example, the effect of different doping processes on the carrier mobility of bottom-up vapor-liquid-solid grown nanowires. Finally, a direct comparison of results from universal mobility analysis of Si nanowires grown under various conditions with established Si MOSFET data would be extremely valuable in assessing the effects of different growth, doping, and post-growth processing on the transport properties of Si nanowires.

ACKNOWLEDGMENTS

This work was supported by the National Science Foundation under Grant No. CMMI-000176. The irradiation and TEM work was supported by the Director, Office of Science, Office of Basic Energy Sciences, Materials Sciences and Engineering Division, of the U.S. Department of Energy under Contract No. DE-AC02-05CH11231. The authors thank Tyler Matthews for helpful discussions. Co-authors from ISOM acknowledge partial funding by national contracts: CAM P2009/ESP-1503, MICINN-PLE2009-0023, and MICINN-MAT-2008-04815, and by the EU under FP7 Contract No. SMASH CP-IP 228999-2.

[1]E. Garnett and P. Yang, Nano Lett. **10**, 1082 (2010).
[2]C. Chan, R. N. Patel, M. J. O'Connell, B. A. Korgel, and Y. Cui, ACS Nano **4**, 1443 (2010).
[3]A. Kolmakov, Y. Zhang, G. Cheng, and M. Moskovits, Adv. Mater. **15**, 997 (2003).
[4]S. Sun and J. Plummer, IEEE T. Electron Dev. **27**, 1497 (1980).
[5]A. C. Ford, J. C. Ho, Y. Chueh, Y. Tseng, Z. Fan, J. Guo, J. Bokor, and A. Javey, Nano Lett. **9**, 360 (2009).
[6]S. A. Dayeh, E. T. Yu, and D. Wang, Small **5**, 77 (2009).
[7]A. Motayed, M. Vaudin, A. V. Davydov, J. Melngailis, M. He, and S. N. Mohammad, Appl. Phys. Lett. **90**, 043104 (2007).
[8]E. Garnett, Y.-C. Tseng, D. R. Khanal, J. Wu, J. Bokor, and P. Yang, Nature Nanotech. **4**, 311 (2009).
[9]E. Koren, J. K. Hyun, U. Givan, E. R. Hemesath, L. J. Lauhon, and Y. Rosenwaks, Nano Letters **11**, 183 (2011).
[10]D. E. Perea, E. R. Hemesath, E. J. Schwalbach, J. L. Lensch-Falk, P. W. Voorhees, and L. J. Lauhon, Nature Nanotech. **4**, 315 (2009).
[11]R. Calarco and M. Marso, Appl. Phys. A **87**, 503 (2007).
[12]R. Calarco, M. Marso, T. Richter, A. I. Aykanat, R. Meijers, A. v. d. Hart, T. Stoica, and H. Luth, Nano Lett. **5**, 981 (2005).
[13]F. Werner, F. Limbach, M. Carsten, C. Denker, J. Malindretos, and A. Rizzi, Nano Lett. **9**, 1567 (2009).
[14]D. R. Khanal and J. Wu, Nano Lett. **7**, 2778 (2007).
[15]A. Sabnis and J. Clemens, IEDM Tech. Dig. (1979), p. 18.
[16]S. Takagi, A. Toriumi, M. Iwase, and H. Tango, IEEE T. Electron Dev. **41**, 2357 (1994).
[17]J. B. McKeon, G. Chindalore, S. A. Hareland, W.-K. Shih, C. Wang, A. F. Tasch, Jr., and C. M. Maziar, IEEE Electr. Dev. Lett. **18**, 200 (1997).
[18]J. Wu, J. Appl. Phys. **106**, 011101 (2009).
[19]G. Brown, J. W. Ager III, W. Walukiewicz, W. J. Schaff, and J. Wu, Appl. Phys. Lett. **93**, 262105 (2008).
[20]D. R. Khanal W. Walukiewicz, J. Grandal, E. Calleja, and J. Wu, Appl. Phys. Lett. **95**, 173114 (2009).
[21]S. X. Li, K. M. Yu, J. Wu, R. E. Jones, W. Walukiewicz, J. W. Ager, W. Shan, E. E. Haller, H. Lu, and W. J. Schaff, Phys. Rev. B **71**, 161201 (2005).
[22]E. Calleja, J. Grandal, M. A. Sánchez-Garcia, M. Niebelschütz, V. Cimalla, and O. Ambachar, Appl. Phys. Lett. **90**, 262110 (2007).
[23]K. Ueno, S. Nakamura, H. Shimotani, A. Ohtomo, N. Kimura, T. Nojima, H. Aoki, Y. Iwasa, and M. Kawasaki, Nature Mater. **7**, 855 (2008). We note that we have never observed any current modulation in MBE grown InN nanowires through a conventional backgate, using both SiO_x and SiN dielectrics of different thicknesses.
[24]R. Jones, S. Li, L. Hsu, K. Yu, W. Walukiewicz, Z. Lillental-Weber, J. Ager III, E. Haller, H. Lu, and W. Schaff, Physica B **376**, 436 (2006).
[25]K. M. Yu, Phys. Stat. Solidi A **206**, 1168 (2009).
[26]R. Jones, "Electrical and Optical Characterization of Group III-Nitride Alloys for Solar Energy Conversion," Ph.D. Thesis, University of California, Berkeley (2008).
[27]W. Hong, G. Jo, J. I. Sohn, W. Park, M. Choe, G. Wang, Y. H. Kahng, M. E. Welland, and T. Lee, ACS Nano **4**, 811 (2010).
[28]G. Jo, W. Hong, J. I. Sohn, M. Jo, J. Shin, M. E. Welland, H. Hwang, K. E. Geckeler, and T. Lee, Adv. Mater. **21**, 2156 (2009).
[29]C. Perkins, Appl. Phys. Lett. **12**, 153 (1968).
[30]D. Neamen, W. Shedd, and B. Buchanan, IEEE Trans. Nucl. Sci. **22**, 2203 (1975).
[31]S. A. Dayeh, D. P. R. Aplin, X. Zhou, P. K. L. Yu, E. T. Yu, and D. Wang, Small **3**, 326 (2007).
[32]L. Hsu, R. E. Jones, S. X. Li, K. M. Yu, and W. Walukiewicz, J. Appl. Phys. **102**, 073705 (2007).
[33]D. R. Khanal and J. Wu, Nano Lett. **7**, 1186 (2007).
[34]M. V. Fischetti, L. Wang, B. Yu, C. Sachs, P. M. Asbeck, Y. Taur, and M. Rodwell, IEDM Elect. Dev. Meeting (2007), p. 109.
[35]The highest fluence (5×10^{15} cm^{-2}) mobility curve requires a reduction in γ to $\sim$1. The cause of this is not fully understood but could be due to the fact that at such high carrier concentrations ($\geq 10^{20}$ cm^{-3}) additional effects such as band renormalization are required to accurately describe the electrostatic behavior of the wire.
[36]K. Lee, J.-S. Choi, S.-P. Sim, and C.-K. Kim, IEEE T. Electron Dev. **38**, 1905 (1991).
[37]M. Maaza, O. Nemraoui, A. C. Beye, C. Sella, and T. Derry, Sol. Energ. Mat. Sol. C **90**, 111 (2006).
[38]G. Kuri, D. Gavillet, M. Döbeli, and D. Novikov, Nucl. Instrum. Meth. B. **266**, 1216 (2008).
[39]J. Grandal, M. A. Sánchez-García, F. Calle, and E. Calleja, Phys. Stat. Sol. C **2**, 2289 (2005).

Downloaded 02 Aug 2011 to 128.32.121.22. Redistribution subject to AIP license or copyright; see http://jap.aip.org/about/rights_and_permissions